Improving efficiency and stability of perovskite solar cells with photocurable fluoropolymers

Federico Bella,[1]† Gianmarco Griffini,[2]*† Juan-Pablo Correa-Baena,[3]† Guido Saracco,[4] Michael Grätzel,[5] Anders Hagfeldt,[3]* Stefano Turri,[2] Claudio Gerbaldi[1]*

Organometal halide perovskite solar cells have demonstrated high conversion efficiency but poor long-term stability against ultraviolet irradiation and water. We show that rapid light–induced free-radical polymerization at ambient temperature produces multifunctional fluorinated photopolymer coatings that confer luminescent and easy-cleaning features on the front side of the devices, while concurrently forming a strongly hydrophobic barrier toward environmental moisture on the back contact side. The luminescent photopolymers re-emit ultraviolet light in the visible range, boosting perovskite solar cells efficiency to nearly 19% under standard illumination. Coated devices reproducibly retain their full functional performance during prolonged operation, even after a series of severe aging tests carried out for more than 6 months.

Photovoltaic devices made with organometal halide perovskites [perovskite solar cells (PSCs)] have achieved certified power con-version efficiencies (PCEs) as high as 22.1%(1–9). Reliable device operation will require achieving long-term stability (*10–12*), in which PSCs suffer from two types of stresses that se-verely limit their operation, namely degradation from atmospheric exposure and electrical stresses (polarization). The latter is represented by a hys-teresis loop in current-voltage measurement un-der light and is caused by ionic motion in the perovskite material that can be overcome largely by using appropriate contacts (*13*) or modifying morphology (*14*). However, the stability of PSCs in humid environments, where photochemical and thermal stresses also are typically encountered, have presented an unsurmountable challenge to date (*11*, *12*).

Several strategies to improve the stability of PSCs have been proposed. Device encapsulation, where hydrophobic polymer layers may substan-tially limit the permeation of atmospheric moisture (15, 16), is not suitable for protecting the device against photochemical and thermal stresses during outdoor functioning. Replacement (or protection) of the organic components with metal oxides—e.g., a chromium oxide-chromium (Cr_2O_3/Cr) interlayer protecting the metal contacts from re-actions with the perovskite material—has recent-ly been proposed, as well as the fabrication of solar cells with all-solution-processed metal oxide charge transport layers (17–19). However, these strategies [and others, such as the perovskite crystal cross-linking with alkylphosphonic acid w-ammonium chlorides (20) or the introduction of porous carbon layers (21, 22)] affect only the air stability of the solar cells. With regard to ul-traviolet (UV)–light stability, cesium bromide has been recently proposed as an interfacial modifier between the electron collection layer and the perovskite absorber layer, but resistance to mois-ture or high temperatures remains to be demon-strated (23).

We propose the use of multifunctional photo-polymers as a comprehensive promising solution to PSC instability. A luminescent downshifting (LDS) fluoropolymeric layer is rapidly photogen-erated on the front side of the device (i.e., the glass side), as detailed in section 1 in the supple-mentary materials (24). The coating prevents the UV portion of the incident solar spectrum from negatively interacting with the PSC stack by converting it into visible light (Fig. 1A) and also increases the photocurrent by 6%. Devices can achieve PCEs approaching 19% without affecting the chemistry as well as the electronic properties of both the photoactive and the buffer layers.

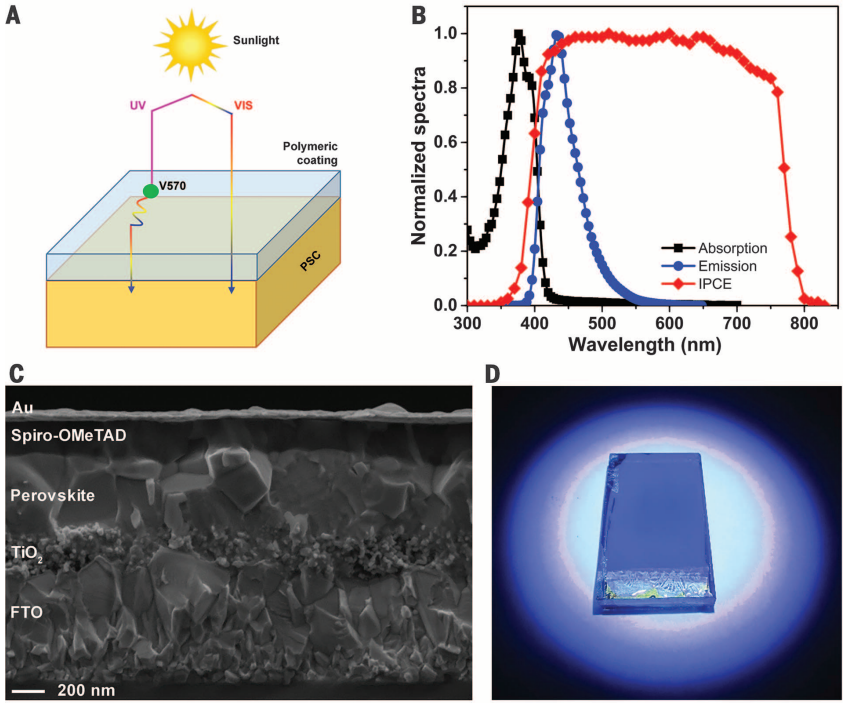

[1]Group for Applied Materials and Electrochemistry (GAME Lab), CHENERGY Group, Department of Applied Science and Technology (DISAT), Politecnico di Torino, Corso Duca degli Abruzzi 24, 10129, Torino, Italy. [2]Department of Chemistry, Materials and Chemical Engineering "Giulio Natta," Politecnico di Milano, Piazza Leonardo da Vinci 32, 20133, Milano, Italy. [3]Laboratory of Photomolecular Science, Institute of Chemical Sciences and Engineering, Ecole Polytechnique Fédérale de Lausanne (EPFL), Chemin des Alambics, Station 3, 1015, Lausanne, Switzerland. [4]Center for Sustainable Futures @PoliTO, Istituto Italiano di Tecnologia, Corso Trento 21, 10129, Torino, Italy. [5]Laboratory of Photonics and Interfaces, Institut des Sciences et Ingénierie Chimiques, Ecole Polytechnique Fédérale de Lausanne (EPFL), Station 3, 1015, Lausanne, Switzerland.
***Corresponding author. Email: federico.bella@polito.it (F.B.); gianmarco.griffini@polimi.it (G.G.); anders.hagfeldt@epfl.ch (A.H.)**
†These authors contributed equally to this work.

Fig. 1. LDS-PSC integrated system. (**A**) Scheme of the UV-coating operating principle. (**B**) Normalized absorption and emission spectra of V570-doped UV coating compared with the IPCE response of the PSC devices under study. (**C**) Cross-sectional field-emission scanning electron microscopy image of the PSC device before coating deposition. (**D**) Digital photograph of a PSC bearing the UV coating when exposed to UV light.

With regard to atmospheric humidity tolerance, a strongly hydrophobic photopolymer is grown on the back contact side. This additional layer behaves as an efficient barrier toward water permeation within the solar cell stack. The resulting devices demonstrated unrivaled stability in terms of PCEs during a 180-day (4320 hours) aging test carried out under different atmospheric conditions and in the presence of various photochemical external stresses. The same devices were also exposed to real outdoor conditions for more than 3 months (2160 hours), successfully demonstrating their exceptional tolerance to dust, soil, and heavy rain on the external glass surface. Finally, the low-surface-energy fluorinated LDS layer makes the front electrode easily cleanable in real outdoor conditions.

The precursor material used for the LDS coatings is based on a combination of a UV-curable chloro-trifluoro-ethylene vinyl ether fluoropolymer binder and a dimethacrylic perfluoropolyether oligomer. The materials react upon UV-light exposure to give a fully cross-linked coating (full characterization of the coating material is presented in sections 2 to 4 in the supplementary materials) (*25*). To impart the LDS functionality to this fluoropolymeric coating (referred to as UV coating hereafter), a luminescent species was added to the precursor formulation in different amounts. The fluorescent organic dye Lumogen F Violet 570 by BASF (referred to hereafter as V570; see inset of fig. S2D) was selected as a luminophore given its commercial availability and favorable optical properties (i.e., high absorption coefficient and fluorescence quantum yield) (*26*). In addition, this particular class of dyes is characterized by relatively good solubility in the polymer to avoid aggregation-induced quenching and easy processability in polymers (*26*).

The optical properties of the V570-doped fluoropolymeric coating are well matched with the spectral response of the PSC devices that we used (Fig. 1B). In particular, the absorption spectrum of the LDS material peaks in the short-wavelength region where the PSC device exhibits a minimum incident photon-to-current conversion efficiency (IPCE) [λ_{max}(abs) = 377 nm]. As a result of the fluorescence process (Fig. 1D), the re-emitted photons are red-shifted to a region where the IPCE of the device is maximum.

We tested these films on devices composed of a typical stack of fluorine-doped tin oxide (FTO)/compact-TiO_2/mesoporous-TiO_2/mixed perovskite/spiro-OMeTAD/gold (Fig. 1C). The compact-TiO_2 and thin mesoporous-TiO_2 layers are used as the electron selective materials, whereas the perovskite capping layer absorbs most of the light and transports the charges. Spiro-OMeTAD is used as the hole selective layer. In this study, a Pb-based "mixed" perovskite containing a mix of cations and halides (formamidinium iodide:PbI_2:methylammonium bromide:$PbBr_2$ = 1.0:1.1:0.20:0.22) is used, as described in our recent publications (*27*, *28*) and detailed in the experimental section. Thin films of liquid, light-curable reactive mixtures (precursors of the fluoropolymeric layer) with different amounts of V570 were spin-coated on the front side of the devices. Then, the as-cast wet fluoropolymeric precursor was UV-irradiated for 30 s under a nitrogen atmosphere to cure a layer ~5 μm in thickness.

The photovoltaic response of the resulting PSCs at increasing V570 concentration is shown in Table 1, where the efficiency-boosting effect of the LDS coatings on device performance can be noted for V570 loadings in the range of 1 to 2 weight % (wt %). The short-circuit photocurrent density (J_{sc}) increased from 19.20 to 20.31 mA cm^{-2} when 2 wt % of V570 was introduced in the fluorinated coating, thus leading to a 6% increase in J_{sc} (and also in PCE). At higher fluorophore loadings (>2 wt %), the photocurrent density started to decrease, likely because a greater amount of fluorescent species can reasonably increase the probability for an emitted photon to be reabsorbed by another adjacent fluorophore molecule within the polymeric layer, given the partial overlap between absorption and emission bands of V570 (Fig. 1B and fig. S1D). For V570 loadings exceeding 3 wt %, the J_{sc} values were further lowered.

To confirm the beneficial effects of the LDS coatings on the photocurrent generated upon illumination, IPCE curves were recorded (Fig. 2A). The luminescent species introduced in the polymeric architecture effectively converted the near-UV region of the solar spectrum (Fig. 2B) into lower-energy photons of wavelengths well matching the absorption spectrum of the perovskite layer.

These PSCs have relatively moderate but highly reproducible efficiencies (≈15.5%). We also investigated the LDS effect with more efficient devices (PCE > 17%) by incorporating an optimized LDS coating (i.e., fluorophore concentration of 2 wt %). The increase in PCE from 17.31 to 18.67% resulted from a ≈5% enhancement in photocurrent (J_{sc} increased from 21.96 to 23.23 mA cm^{-2}). Given the correlation between J_{sc} and V570 content (Table 1) and the broadening of the IPCE curve in the UV region (see Fig. 2B), we can exclude that such photocurrent enhancement is caused by a mere antireflective effect produced by the LDS layer (as also confirmed by the poorer performance observed on the undoped LDS system). Conversely, the downshifting phenomenon consistently explains the measured trends. The integration of the product of the AM1.5G photon flux with the IPCE spectrum (Fig. 3B) yielded predicted J_{sc} values equal to 21.09 and 22.13 mA cm^{-2} for the uncoated and coated devices, respectively; the mismatch with respect to the values inferred

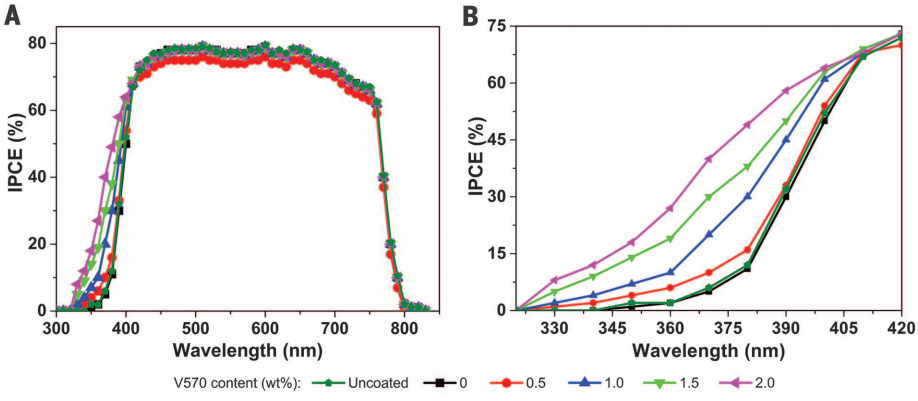

Fig. 2. IPCE curves for PSCs. (**A**) Cells were coated with the LDS fluoropolymeric layer loaded with different amounts (0 to 2 wt %) of V570. (**B**) Detail of IPCE curves for illumination below 420 nm. Mask area = 0.16 cm^2.

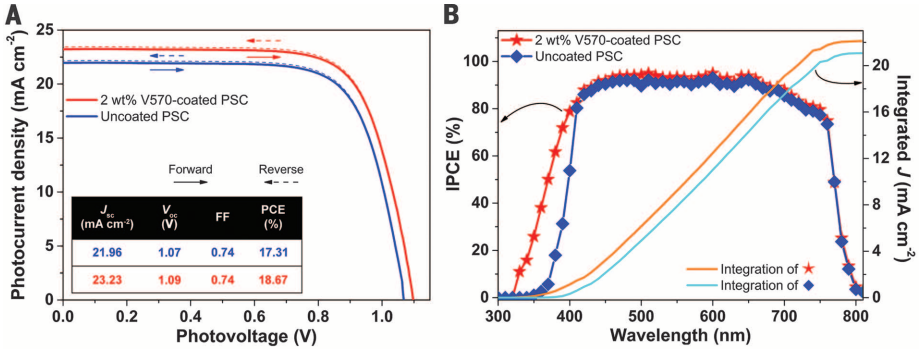

Fig. 3. Photovoltaic characterization of the best device. (**A**) *J-V* curves (1 Sun, AM1.5G, 5 mV s^{-1}) for a highly efficient PSC before and after coating with the optimized LDS fluoropolymeric layer (2 wt % V570). Dotted lines represent the reverse scan. (**B**) IPCE curves of the same PSCs. The integration of the product of the AM1.5G photon flux with the IPCE spectrum is also shown for coated and uncoated devices.

from the photocurrent density versus voltage (*J-V*) curves (Fig. 3A) was equal to ≈1 mA cm^{-2}, consistent with other recent reports in the PSC field (*21*, *29*, *30*). The excellent quality of the fabricated PSCs is reflected in the negligible hysteresis phenomenon observed in the *J-V* curves of our high-efficiency devices (Fig. 3A, dotted lines), consistent with recent reports (*14*).

We investigated whether these luminescent polymeric coatings (with 2 wt % loading) can enhance device stability on a long-term basis by carrying out three aging studies under markedly different conditions. In the first aging test, uncoated devices and front-coated ones (five solar cells for each condition) were studied for an overall period of 6 months. In the first 3 months, the devices were kept in an Ar-filled dry glove box and continuously irradiated (8 hours per day) with a UV optical fiber having a 5 mW cm^{-2} intensity. This value simulates well the 5% contribution given by UV light (280 to 400 nm) to the overall solar spectral irradiance on Earth (1000 W m^{-2}, AM1.5G) based on the Standard Reference Solar Spectra (ASTM G-173-03). The uncoated devices (black curve) in this UV-induced aging test (Fig. 4A) lost 30% of their initial efficiency after 1 week of exposure and failed after 1 month; conversely, all five front-coated cells (red curve) demonstrated excellent stability under the same conditions, retaining 98% of their initial PCE after 3 months.

After this period, the solar cells were taken out of the Ar-filled glove box and placed inside a quartz chamber, where they were exposed to constant relative humidity (RH) (50%), and the aging test was allowed to proceed in the same UV irradiation conditions described above. Figure 4A shows that, immediately after the modification of the aging conditions, front-coated cells (red curve) showed a sharp decrease in efficiency, resulting in an 82% decrease of their initial efficiency at the end of the second quarter of the aging test. Such a rapid decay was attributed to the amount of moisture present in the aging chamber that progressively infiltrated the PSC stack from the back contact side, thus causing the gradual hydrolysis of the perovskite layer. The effects of degradation were easily detectable by simple visual inspection, as a progressive yellowing of the mixed-perovskite layer upon 50% RH exposure was observed (see inset of Fig. 4A).

With the aim of stabilizing our devices in terms of photochemical resistance, as well as moisture tolerance, a fluoropolymeric light-curable coating was deposited also on the back contact side (front/back-coated device configuration). The same formulation used in the LDS experiment was used for back-coating the PSC devices, except that no luminescent dye was used. The use of such fluoropolymeric layer on top of the PSC stack is expected to efficiently combat water permeation through the top back contact toward the perovskite layer as a result of the highly hydrophobic character of the coating (see section 3 in the supplementary materials) (*25*). In addition, the cross-linked nature of the fluoropolymeric UV coating entails a lower free volume than typical non–cross-linked polymeric systems and should therefore enhance the long-term durability of PSCs (*31*, *32*).

Figure 4A shows the aging test performed onto front/back-coated PSCs (blue curve), i.e., devices bearing the luminescent coating on the front side and the moisture-resistant one on the back contact side. All of the five devices maintained an excellent stability (98%) in the aging conditions resulting from the combined effects

Table 1. Photovoltaic parameters of PSCs coated with the fluoropolymeric layer laden with different amounts (0 to 3 wt %) of V570. Average values for uncoated devices are also shown for comparison purposes. Each experimental condition was reproduced five times on different devices; solar cells were tested under 1 Sun, AM1.5G, at a scan rate of 5 mV s^{-1} and with a mask area of 0.16 cm^2. In addition to the J_{sc} trend described in the text, a slight variation of V_{oc} (open-circuit voltage) values can also be appreciated, scaling logarithmically with J_{sc} in accordance with the photodiode equation—i.e., $V_{oc} = kTq^{-1}ln(J_{sc}J_0^{-1} + 1)$. FF, fill factor.

V570 (wt %)	J_{sc} (mA cm^{-2})	V_{oc} (V)	FF	PCE (%)	ΔPCE (%)
Uncoated	19.20 ± 0.05	1.120 ± 0.003	0.72 ± 0.01	15.48	0
0	18.14 ± 0.05	1.108 ± 0.003	0.72 ± 0.01	14.47	-6.52
0.5	18.52 ± 0.04	1.111 ± 0.002	0.73 ± 0.01	15.02	-3.54
1	19.37 ± 0.06	1.123 ± 0.003	0.72 ± 0.01	15.66	+0.89
1.5	19.90 ± 0.05	1.133 ± 0.003	0.72 ± 0.01	16.23	+3.65
2	20.31 ± 0.04	1.142 ± 0.002	0.73 ± 0.01	16.93	+5.78
2.5	20.20 ± 0.06	1.137 ± 0.003	0.72 ± 0.01	16.54	+5.21
3	20.11 ± 0.08	1.134 ± 0.004	0.73 ± 0.01	16.65	+4.74

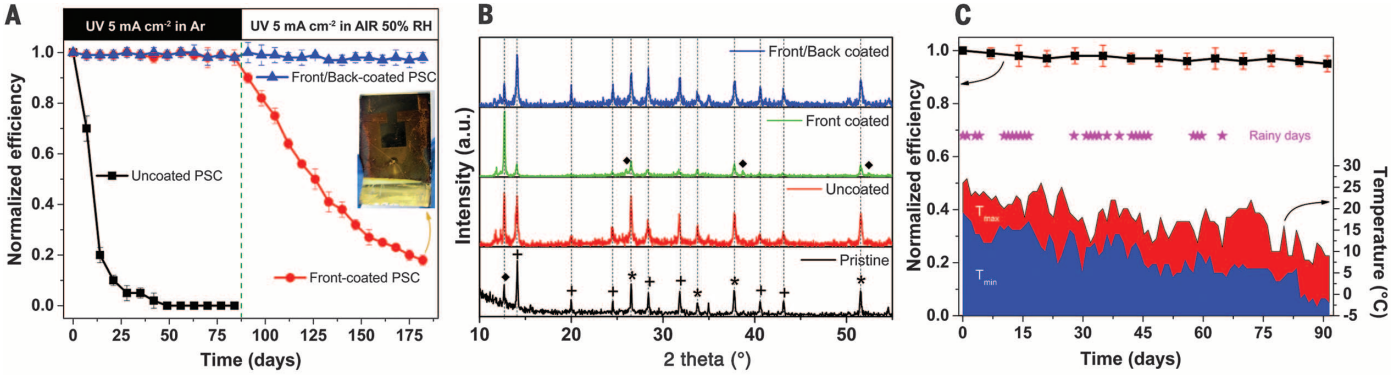

Fig. 4. Aging of LDS-PSC integrated system. (**A**) Results of the aging test on the three series of PSCs: uncoated, front-coated (i.e., luminescent fluorinated coating on the front side), and front/back-coated (i.e., front side coated with the luminescent fluorophore and back contact coated with the moisture-resistant fluoropolymeric layer). During the first 3 months, PSCs were kept under Ar atmosphere and in the next 3 months under air at 50% RH, in both cases under continuous UV irradiation. PCE was measured once a week. A digital photograph of a front-coated solar cell at the end of the test is also shown. Further details are given in fig. S1A and section 5 in the supplementary materials. (**B**) XRD patterns of both uncoated and (front and front/back) coated PSC devices after the 6 months aging test. For comparison purposes, the XRD pattern of the pristine uncoated PSC system is also shown. Asterisks, crosses, and diamonds denote the main signals ascribed to FTO, perovskite, and PbI_2, respectively. (**C**) Results of the aging test on front/back coated devices left for three months on the terrace of the Politecnico di Torino building in Turin (Italy), thus experiencing real outdoor operating conditions. PCE was measured once a week. Further details are given in fig. S1B and section 7 in the supplementary materials.

of photochemical and environmental stresses. X-ray diffraction (XRD) (Fig. 4B) analysis showed that performance degradation corresponded to the decomposition of the crystalline perovskite material into PbI_2, which was not observed for the fully coated devices (see section 6 in the supplementary materials).

Given the stabilizing effect of the fluoropolymeric coating applied on both sides of the cells, a second aging test was designed to verify the stability of the front/back-coated PSCs under real outdoor atmospheric conditions, where temperature variations, precipitation phenomena, and pollution are typically encountered. A batch of five cells was exposed on the terrace of the Politecnico di Torino building in Turin (45°06′N, 7°66′E), located in northwest Italy, in a humid subtropical climate zone from October to December 2015. The PSCs were subjected to highly variable climatic conditions, as outdoor temperatures ranged from −3° to +27°C, and 27 out of 92 days were characterized by heavy rain and storms (*33*), as shown in Fig. 4C. The front/back-coated PSCs exhibited long-term stability retaining 95% of their initial efficiency after this test by (i) protecting the perovskite from UV radiation, converting it into exploitable visible photons; (ii) acting as a moisture barrier, thus preventing hydrolytic phenomena of the perovskite material; and (iii) keeping the front electrode clean by means of the easy-cleaning characteristics of this fluorinated polymer. Similar results were found for outdoor tests performed during Summer 2016, and the data collected are available in section 7 in the supplementary materials.

To demonstrate the water resistance of the photopolymerized fluorinated coatings, we kept five solar cells for 1 month in a closed chamber in the presence of a beaker containing boiling water (95% RH, fig. S1C), and the photovoltaic response was evaluated once a week. After 1 month, four of the five cells withstood the strong aging conditions and remarkably retained 96 ± 2% of their initial PCE. Only one device lost 95% of its initial efficiency after the first week. After inspection, we found a small area on the back side of the solar cell not thoroughly coated by the fluoropolymeric layer. The nonhomogeneous deposition of the coating caused a gradual hydrolysis of the underlying perovskite layer. We also dipped the front/back-coated devices into water. After 1 day of immersion, no changes in their photovoltaic performance were observed.

REFERENCES AND NOTES

1. H. S. Kim *et al*., *Sci. Rep.* **2**, 591 (2012).
2. M. M. Lee, J. Teuscher, T. Miyasaka, T. N. Murakami, H. J. Snaith, *Science* **338**, 643–647 (2012).
3. H. Zhou *et al*., *Science* **345**, 542–546 (2014).
4. M. Liu, M. B. Johnston, H. J. Snaith, *Nature* **501**, 395–398 (2013).
5. J. Burschka *et al*., *Nature* **499**, 316–319 (2013).
6. National Center for Photovoltaics (NCPV) at the National Renewable Energy Laboratory (NREL); http://www.nrel.gov/ncpv (accessed July 2016).
7. N. G. Park, *Mater. Today* **18**, 65–72 (2015).
8. J. Seo, J. H. Noh, S. I. Seok, *Acc. Chem. Res.* **49**, 562–572 (2016).
9. H. S. Jung, N. G. Park, *Small* **11**, 10–25 (2015).
10. T. A. Berhe *et al*., *Energy Environ. Sci.* **9**, 323–356 (2016).
11. Y. Rong, L. Liu, A. Mei, X. Li, H. Han, *Adv. Energy Mater.* **5**, 1501066 (2015).
12. T. Leijtens *et al*., *Adv. Energy Mater.* **5**, 1500963 (2015).
13. J. P. Correa Baena *et al*., *Energy Environ. Sci.* **8**, 2928–2934 (2015).
14. J. P. Correa-Baena *et al*., *Adv. Mater.* **28**, 5031–5037 (2016).
15. H. C. Weerasinghe, Y. Dkhissi, A. D. Scully, R. A. Caruso, Y. B. Cheng, *Nano Energy* **18**, 118–125 (2015).
16. I. Hwang, I. Jeong, J. Lee, M. J. Ko, K. Yong, *ACS Appl. Mater. Interfaces* **7**, 17330–17336 (2015).
17. M. Kaltenbrunner *et al*., *Nat. Mater.* **14**, 1032–1039 (2015).
18. J. You *et al*., *Nat. Nanotechnol.* **11**, 75–81 (2016).
19. K. Domanski *et al*., *ACS Nano* **10**, 6306–6314 (2016).
20. X. Li *et al*., *Nat. Chem.* **7**, 703–711 (2015).
21. A. Mei *et al*., *Science* **345**, 295–298 (2014).
22. L. Zhang *et al*., *J. Mater. Chem. A* **3**, 9165–9170 (2015).
23. W. Li *et al*., *Energy Environ. Sci.* **9**, 490–498 (2016).
24. Materials and methods are available as supplementary materials on *Science* Online.
25. F. Bella *et al*., *Adv. Funct. Mater.* **26**, 1127–1137 (2016).
26. L. R. Wilson, B. S. Richards, *Appl. Opt.* **48**, 212–220 (2009).
27. D. Bi *et al*., *Sci. Adv.* **2**, e1501170 (2016).
28. F. Giordano *et al*., *Nat. Commun.* **7**, 10379 (2016).
29. D. Liu, T. L. Kelly, *Nat. Photonics* **8**, 133–138 (2014).
30. J.-H. Im, I.-H. Jang, N. Pellet, M. Grätzel, N.-G. Park, *Nat. Nanotechnol.* **9**, 927–932 (2014).
31. G. Griffini, M. Levi, S. Turri, *Sol. Energy Mater. Sol. Cells* **118**, 36–42 (2013).
32. G. Griffini, M. Levi, S. Turri, *Prog. Org. Coat.* **77**, 528–536 (2014).
33. Il Meteo; http://www.ilmeteo.it/meteo/Torino (accessed September 2016).

ACKNOWLEDGMENTS

Authors from EPFL thank the Swiss National Science Foundation, the NRP 70 "Energy Turnaround," the 9th call proposal 906 (CONNECT PV), SNF-NanoTera, and the Swiss Federal Office of Energy (SYNERGY) for financial support. All data used in this study are included in the main text and in the supplementary materials.

SUPPLEMENTARY MATERIALS

www.sciencemag.org/content/354/6309/203/suppl/DC1
Materials and Methods
Supplementary Text Sections 1 to 7
Figs. S1 to S8
References (*34*–*40*)

21 June 2016; accepted 20 September 2016
Published online 29 September 2016
10.1126/science.aah4046